

MALAYSIAN JOURNAL OF ANALYTICAL SCIENCES

Journal homepage: https://mjas.analis.com.my/



Research Article

Theoretical investigation of electronic and non-linear optical properties of new D- π -A compounds: A TD-DFT approach

Said Kerraj^{1*}, Ahmed Arif², Younes Rachdi¹, Said Zouitina¹, Mohammed El idrissi², and Said Belaaouad¹

¹Laboratory Physical Chemistry of Materials, Department of chemistry, Faculty of Sciences Ben M'Sik, University Hassan II, Casablanca, Morocco

²Team of Chemical Processes and Applied Materials, Faculty Polydisciplinary Sultan Moulay Slimane University, Beni-Mellal Morocco

Received: 28 August 2024; Revised: 4 December 2024; Accepted: 6 January 2025; Published: 24 April 2025

Abstract

This study evaluates the electronic structure, charge transfer properties, and non-linear optical (NLO) potential of five new organic dyes with a Donor- π -Acceptor (D- π -A) structure, containing the commonly used anchoring group, cyanoacrylic acid. DFT/B3LYP calculations were carried out using a 6-31G(d,p) basis set. The optimized geometries indicate many frontiers molecular orbitals with energy gaps ranging from 1.766 to 2.717 eV, with MK162 having the lowest bandgap, making it a promising option for organic solar cells. Natural bond orbital (NBO) study reveals extensive electron delocalization, demonstrating strong donor-acceptor interactions within each molecule, notably for MC20 and MK162, with high stabilization energies indicating significant charge transfer properties. The Mulliken charge distribution shows that sulfur has a positive charge, while the carbon atoms that are close to sulfur have negative charges, which facilitates charge transfer. Furthermore, MK162 has the greatest levels of polarizability, hyperpolarizability, and dipole moments among the molecules examined by NLO analysis, making it the most promising of the group. These results support the possibility that these organic dyes might be useful options for organic solar cells.

Keywords: Donor–π–Acceptor, TD-DFT, NLO, NBO, intramolecular charge transfer

Introduction

With the increasing demand for more efficient optoelectronic materials, the research focus on Non-Linear Optical (NLO) materials has grown rapidly in recent years. Various practical and theoretical studies have been conducted in this field. with a particular interest in organic compounds possessing NLO characteristics. The versatility of these materials extends across various domains, encompassing applications in second harmonic generation (SHG) photonics [1], electro optics (EO) processes [2], telecommunications [3], data storage [4], and biological applications [5]. NLO materials could change the frequency of the incident laser when they interact. To improve the NLO response, much research has been conducted on electrooptical materials using various approaches [6, 7]. These approaches include molecular systems with extended π -electron structures, twisted π -electron structures, donor- π -acceptor (D- π -A) models, octupolar molecules, bond length alternation theory, enhanced push-pull properties, and metal ligands in organic compounds [8, 9, 10]. The NLO properties are determined by the extent of charge transfer (TC) interaction through conjugative pathways and the electron transfer capacity of an aromatic ring, as well as its ionization potential (PI) and electron affinity (AE) [11, 12].

Linear polarization ($\Delta\alpha$) and first-order hyperpolarization (β) are necessary for rationally designing optimized materials for photonic devices such as and total-optical electro-optical modulators commutators [13, 14]. The most frequently mentioned organic small molecules typically adopt a variety of arrangements, including D- π -A, D-A-D, D- π -D, A- π -A, and D- π -A- π -D, to boost the efficiency of intramolecular charge transfer (ICT) and permit electron injections from the excited molecule to the acceptor [15,16]. Due to their exceptional optical properties, D- π -A pushpull models have received a lot of attention in organic materials chemistry [17, 18]. These compounds have a unique molecular architecture,

^{*}Corresponding author: Krjsaid@gmail.com

with an electron donor (D) coupled to an electron acceptor (A) via an extended π -system. The D- π -A configuration promotes electron delocalization across the molecule, allowing for efficient light absorption at a wide range of wavelengths [19, 20]

This article focuses on the development of a novel class of organic electron donor compounds designed for application in organic photovoltaic cells. Through a comprehensive computational investigation employing B3LYP and time-dependent density functional theory (TD-DFT), we present the characterization of a series of novel compounds, namely MC28, MC20, MZ173, MZ175, and MK162 (**Table 1**). The research integrates experimental and computational results, demonstrating a consistent alignment between the

molecular structure and its electronic properties with theoretical predictions.

Building on the foundation of previous studies, this work explores the unique features of these modified molecules, shedding light on their potential in enhancing the performance of organic photovoltaic cells. The investigation delves into key aspects such as the electronic structure, dipole moment, first-order hyperpolarization, gap energy, electronic affinity, electronegativity, chemical potential, chemical hardness, softness, and electrophilicity index, employing TD-DFT calculations. The subsequent sections of this article delve deeper into the specifics of these findings, providing valuable insights into the potential of these novel organic compounds for advancing the field of organic photovoltaics.

Table 1. Designed molecular structures (MC28, MC20, MZ173, MZ175 and MK162)

Computational Methods

The theoretical calculation method is critical for modeling the structure of the organic dyes and determining its molecular characteristics [21]. The TD-DFT calculations were performed using Gaussian09 software and the correlation exchange functional B3LYP with Gaussian basis 6-31G for the optimization of the proposed molecules with titles MC28, MC20, MZ173, MZ175, and MK162 [22, 23]. The optimized structure was visualized with Gauss View 6.0.16. The experimental and computational data converge to show that the molecular structure and its electronic properties are coherent with the theoretical predictions, as anticipated. During the geometry optimization process, no symmetrical constraints were used [21]. Additionally, the following equations were used to compute the values of the total dipole moment (µ), the average polarizability (α) , and the first order hyperpolarizability (β) The values of α and β in atomic units (a.u.) have been transformed to electrostatic units (esu) according to the relationship (α ; 1a.u = 0.1482×10⁻²⁴ esu, β ; 1a.u = 8.6393×10⁻³³). These parameters can be used in certain equations, giving as follows [25, 26].

The dipole moment was identified by:

$$\mu = \left(\mu_a^2 + \mu_y^2 + \mu_z^2\right)^{\frac{1}{2}} \tag{1}$$

The polarizability is determined by:

$$<\alpha> = \frac{1}{3} \left(\alpha_{xx} + \alpha_{yy} + \alpha_{2z}\right) \tag{2}$$

The expression for the first-order hyperpolarizability is:

$$\beta_{tot} = (\beta_x^2 + \beta_y^2 + \beta_z^2)^{\frac{1}{2}}$$
 (3)

Where β_x β_y , and β_z are provided by

$$\beta_{x} = (\beta_{xxx} + \beta_{xyy} + \beta_{xzz})^{2}$$

$$\beta_{y} = (\beta_{yyy} + \beta_{yzz} + \beta_{yxx})^{2}$$

$$\beta_{z} = (\beta_{zzz} + \beta_{zxx} + \beta_{zyy})^{2}$$

$$(4)$$

Equation (3) can be rewritten as follows, using equation (4):

$$\beta_{y} = \left[\left(\beta_{xxx} + \beta_{xyy} + \beta_{xzz} \right)^{2} + \left(\beta_{yyy} + \beta_{yzz} + \beta_{yxx} \right)^{2} + \left(\beta_{zzz} + \beta_{zxx} + \beta_{zyy} \right)^{2} \right]$$
(5)

The global reactivity parameters of a molecule can be calculated using the energies of its HOMO and LUMO orbitals.

The chemical potential (m), global hardness (η), softness (S), global electrophilicity index (ω), electron affinity (EA), ionization potential (IP), and electronegativity (v) are all expressed as equations in [27, 28, 29].

$$m = \frac{(EHOMO + ELUMO)}{2} \tag{6}$$

$$\eta = \frac{I - A}{2} \tag{7}$$

$$S = \frac{1}{2\eta} \tag{8}$$

$$\omega = \frac{\mu^2}{2\eta} \tag{9}$$

$$AE = -E_{LUMO} \tag{10}$$

$$I = -E_{HOMO} \tag{11}$$

$$\chi = \frac{I+A}{2} \tag{12}$$

Results and Discussion

Structural geometry and molecular frontier orbitals

Figure 1 shows the optimized molecular geometries of stable compounds obtained by B3LYP calculations using the 6-31G(d,p) base group. The various geometric parameters are shown in Table 2. The reactivity of organic compounds and the nature of their intramolecular charge transfer (ICT) can be determined by frontier molecular orbital (FMO) analysis. Molecular frontier orbitals (FMOs) are essential for understanding the reactivity of organic compounds. The most occupied molecular orbital (HOMO) characterizes the electron-rich region, while the least occupied molecular orbital (LUMO) represents the electron-poor region [30]. Table 2 illustrates the energies of HOMO, LUMO and the energy gap (E_{gap}) .

The bandgap energies of the studied compounds range from 1.766 to 2.7171 eV and are classified as follows: $E_{gap}(MK\ 162) > E_{gap}(MZ\ 175) > E_{gap}(MZ\ 173) > E_{gap}\ (MC\ 20) > E_{gap}\ (MC\ 28).$ Mk162 has the lowest gap energy compared to other molecules, indicating its potential as a very favorable candidate for use in organic heterojunction solar cells, to more effectively demonstrate the disparity in energy gaps, the HOMO and LUMO frontier orbitals for each molecule have been illustrated in **Figure 2**.

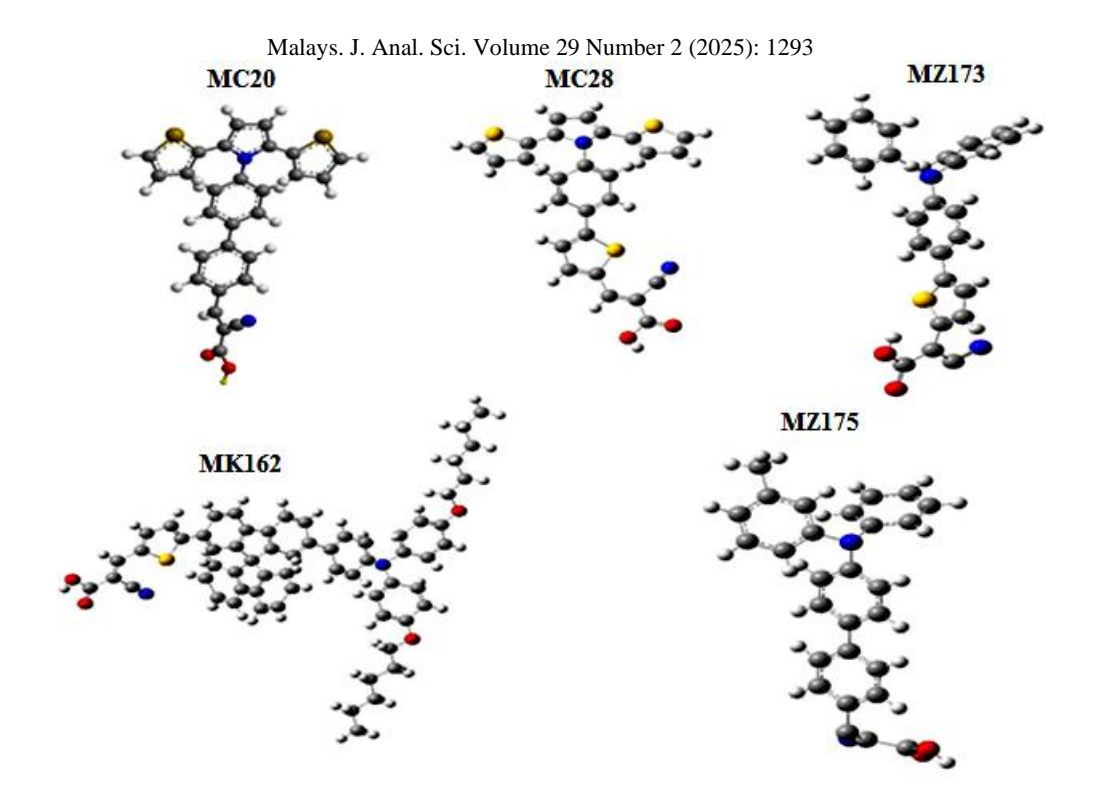


Figure 1. The optimized structures of the investigated molecules

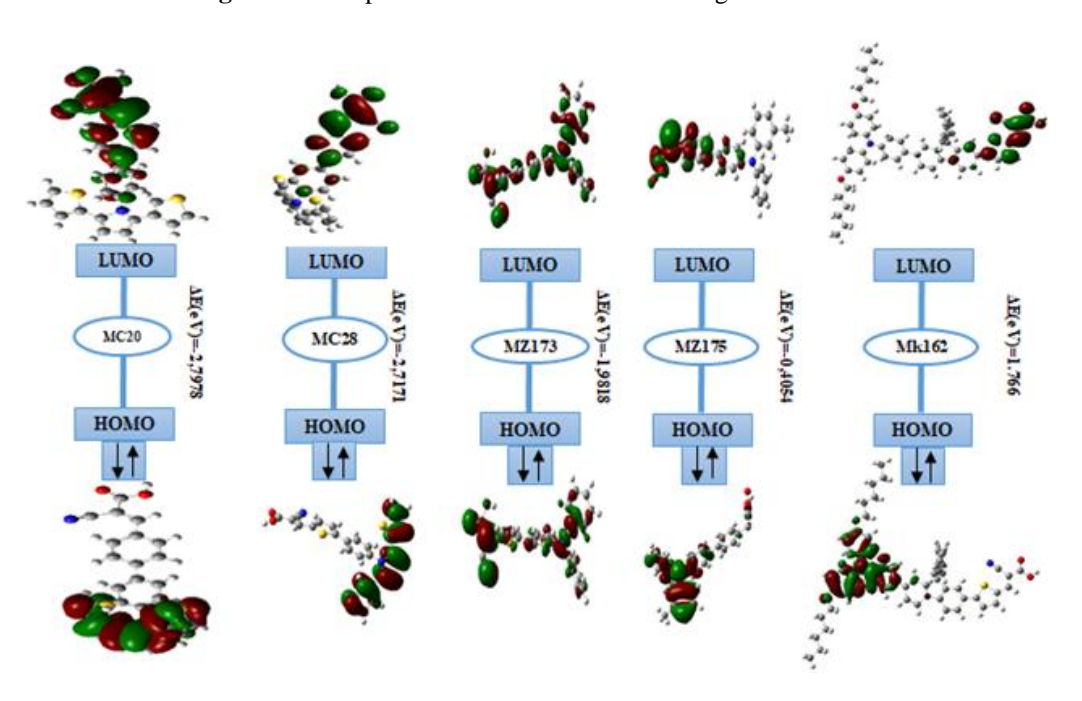


Figure 2. Optimized molecular frontier orbitals of designed molecules MC20, MC28, MK1623, MZ175 and MZ173 based on DFT/B3LYP 6-31G(d,p)

Natural bond orbital (NBO) analysis

The (NBO) study is an important tool for understanding the intramolecular and intermolecular bond interactions that cause electron density delocalization and charge transfer in molecular systems. Thus, all possible interactions between filled Lewis bonds (donors) and empty non-Lewis bonds (acceptors), by

estimating their energetic importance through second-order perturbation theory $E^{(2)}$ [34, 35]. Since these interactions lead to an occupancy donor for the localized NBO of the idealized Lewis structure in the empty non-Lewis orbitals. For each donor (i) and acceptor (j) NBO, the stabilization energy $E^{(2)}$ associated with electron

delocalization between donor and acceptor is expressed according to the following equation:

$$E^{(2)} = \Delta E_{ij} = q_i \frac{(F_{ij})^2}{\varepsilon_i - \varepsilon_i}$$
 (13)

where q_i is the donor orbital occupancy, ϵ_i and ϵ_j are diagonal elements (orbital energies) and $F_{i,j}$ is the fock matrix element and $E^{(2)}$ is stabilization energy [36].

The stabilization energy $E^{(2)}$ is proportional to the interaction intensities of the NBOs, so a large value of $E^{(2)}$ shows an intensive interaction between the donor orbital, which has a greater tendency to supply an electron, and the acceptor orbital, which has a greater tendency to accept an electron, and the degree of electron delocalization is higher [37].

The major results of the NBO calculations for the molecules MC20, MC28, MK162, MZ173 and MZ175, carried out with the NBO 3.1 program integrated into Gaussian 09 using B3LYP/6-31G, are given in Table 2 The numbering of the molecules studied is shown in Figure 1. The most likely transition obtained for the MC20 molecule is LP3(O31) to LP*1(H32) with a huge stabilization energy 476.90 kcal/mol, which offers high stabilization and represents a strong interaction between donor (LP3) and acceptor (LP*1). Other transitions such as π (C25-C26) \rightarrow $\pi^*(C28-C29), \quad \pi(C28-C29) \rightarrow \pi^*(C33-N34),$ $\pi(C28-C29) \rightarrow \pi^*(C30-O35)$ and $\pi(C33-N34) \rightarrow$ $\sigma^*(C24-H49)$ with very close energies 35.26, 35.02, 41.57 and 46. 25 kcal/mol respectively. In addition, electron delocalization from $\pi^*(C25$ -C26) to $\pi^*(C23-C24)$ and $\pi^*(C16-C21)$ to $\pi^*(C19-C20)$ with huge stabilization energy 244.86 and 301.07 kcal/mol respectively.

For the MC28 molecule the most likely transition observed is LP1(C19) to $\pi^*(C22\text{-C31})$ with a huge stabilization energy 103.21 kcal/mol, which offers great stabilization and represents a strong interaction between donor (LP1) and acceptor (π^*) . Other transitions such as $\pi(C17\text{-C18}) \rightarrow$ LP1(C19), $\pi(C20\text{-C21}) \rightarrow$ LP1(C19), $\pi^*(C22\text{-C31}) \rightarrow$ LP1(C19), LP1(C19) \rightarrow $\pi^*(C17\text{-C18})$ and LP1(C19) \rightarrow $\pi^*(C20\text{-C21})$ with various energies 45.95, 44.22, 43.76, 70.87 and 72. 72 kcal/mol respectively. In addition, electron delocalization from $\pi^*(N5\text{-C16})$ to $\pi^*(C17\text{-C18})$ and $\pi^*(N5\text{-C16})$ to $\pi^*(C20\text{-C21})$ with higher stabilization energies 136.56 and 147.11 kcal/mol respectively.

For the MK162 molecule the most likely transition obtained is LP3(O57) to LP*1(H58) with a huge stabilization energy 478.36 kcal/mol, which offers great stabilization and represents a strong

interaction between donor (LP3) and acceptor (LP*1). Other transitions such as $\pi(C52\text{-}C53) \rightarrow \pi^*(C54\text{-}O71)$, $\pi(C61\text{-}C63) \rightarrow \pi^*(C62\text{-}C66)$, LP1(N14) $\rightarrow \pi^*(C28\text{-}C29)$ and LP2(O57) $\rightarrow \pi^*(C54\text{-}O71)$ with various energies 40.53, 54.00, 64.93 and 50. 39 kcal/mol respectively, in addition, electron delocalization from $\pi^*(C28\text{-}C29)$ to $\pi^*(C30\text{-}C31)$ and $\pi^*(C30\text{-}C31)$ to $\pi^*(C34\text{-}C39)$ with higher stabilization energies 229.57 and 220.38 kcal/mol respectively.

For the MZ173 molecule the most likely transition to be noticed is LP1(N7) to LP*1(C8) with a huge stabilization energy 145.46 kcal/mol, which offers great stabilization and represents a strong interaction between donor (LP1) and acceptor (LP*1). Other transitions such as π (C15-C16) \rightarrow $LP*1(C8), \pi(C18-C19) \rightarrow LP*1(C8), LP1(C17)$ $\to \pi^*(C15\text{-}C16)$, LP1(C17) $\to \pi^*(C18\text{-}C19)$ and LP1(C17) $\rightarrow \pi^*$ (C21-C22) with varying energies 59.05, 56. 61, 77.79, 79.99 and 105.05 kcal/mol respectively. In addition, electron delocalization from $\pi^*(C9-C14)$ to $\pi^*(C12-C13)$ with higher stabilization energy 231.44 kcal/mol respectively. For the MZ175 molecule the most likely transition observed is LP1(C23) to π^* (C26-C27) with a largest stabilization energy value 91.50 kcal/mol, which offers great stabilization and represents a strong interaction between donor (LP1) and acceptor (π^*) . Other transitions such as $\pi(C17$ -C18) \to LP*1(C20), π (C21-C22) \to LP*1(C20), $\pi(C24-C25) \to LP*1(C20), LP1(C23) \to \pi*(C21-$ C22), LP1(C23) $\rightarrow \pi^*$ (C24-C25) with varying energies 57.18, 54.46, 52.70, 74.38 and 75. 47 kcal/mol respectively. In addition, electron delocalization from $\pi^*(C8-C19)$ to $\pi^*(C15-C16)$ and $\pi^*(C9-C14)$ to $\pi^*(C10-C11)$ with a huge stabilization energy of around 327.97 and 289.42 kcal/mol respectively.

Furthermore, the results clearly show that the delocalization of π electrons from C-C bonding orbitals to their anti-bonding π^* orbitals, of LP electrons from C atom orbitals to anti-bonding π^* C-C bonding orbitals, of LP electrons from O atom orbitals to LP* of H atom orbitals and of LP electrons from N atom orbitals to LP* of C atom orbitals promotes molecule stabilization. Although the presence of conjugation along the studied molecules is quite clear by the transitions $\pi^*(\text{C-C}) \to \pi^*(\text{C-C})$ and $\pi^*(\text{N-C}) \to \pi^*(\text{C-C})$.

Consequently, our NBO calculations indicate that intramolecular interactions and extended hyperconjugation provide more stability and an important explanation for charge transfer properties in the five compounds studied. As a result, they may be useful for potential NLO features.

Malays. J. Anal. Sci. Volume 29 Number 2 (2025): 1293 **Table 2.** NBO analysis data for MC20, MC28, MK162, MZ173 and MZ175 molecules obtained by B3LYP/31-G

					E(2)	E(j)-E(i)	F(i,j)
	Donor (i)	Type	Acceptor (j)	Type	kcal/mol	a.u.	a.u.
	C 1 - C 2	π	C 3 - C 4	π^*	18.42	0.29	0.068
	C3 - C4	π	C 1 - C 2	π^*	18.48	0.29	0.068
	C 16 - C 21	π	C 19 - C 20	π^*	20.55	0.29	0.070
	C 17 - C 18	π	C 16 - C 21	π^*	21.88	0.27	0.071
	C 17 - C 18	π	C 19 - C 20	π^*	19.05	0.29	0.068
	C 19 - C 20	π	C 16 - C 21	π^*	20.06	0.27	0.066
	C 19 - C 20	π	C 17 - C 18	π^*	20.48	0.27	0.069
	C 19 - C 20	π	C 22 - C 27	π^*	28.63	0.28	0.079
	C 22 - C 27	π	C 19 - C 20	π^*	21.88	0.29	0.071
	C 22 - C 27	π	C 25 - C 26	π^*	25.19	0.27	0.074
	C 23 - C 24	π	C 22 - C 27	π^*	25.18	0.28	0.075
	C 25 - C 26	π	C 23 - C 24	π^*	19.83	0.29	0.071
	C 25 - C 26	π	C 28 - C 29	π^*	35.26	0.28	0.092
	C 28 - C 29	π	C 25 - C 26	π^*	15.77	0.31	0.065
	C 28 - C 29	π	C 30 - O 35	π^*	41.57	0.27	0.096
	C 28 - C 29	π	C 33 - N 34	π^*	35.02	0.36	0.104
MC20	C 33 - N 34	π	C 24 - H 49	σ^*	46.25	0.95	0.188
MC20	S 10	LP 2	C 6 - C 7	π^*	25.12	0.26	0.073
	S 10	LP 2	C 8 - C 9	π^*	23.09	0.26	0.071
	S 15	LP 2	C 11 - C12	π^*	25.41	0.26	0.073
	S 15	LP 2	C13 - C 14	π^*	23.11	0.26	0.071
	O 35	LP 2	C 29 - C 30	σ^*	15.90	0.87	0.108
	O 35	LP 2	C 30 - O 31	σ^*	32.81	0.59	0.125
	C 16 - C 21	π^*	C 19 - C 20	π^*	301.07	0.01	0.082
	C 25 - C 26	π^*	C 23 - C 24	π^*	244.86	0.01	0.083
	C 28 - C 29	π^*	C 33 - N 34	π^*	49.65	0.05	0.095
	C 30 - O 35	π^*	C 28 - C 29	π^*	83.76	0.04	0.089
	O 31	LP 3	H 32	LP*1	476.90	0.64	0.494
	O 31	LP 3	H 32	RY*1	30.51	1.13	0.191
	H 32	LP*1	H 32	RY*1	64.08	0.49	0.318
	C 1-C 2	π	C 3-C 4	π^*	18.59	0.29	0.068
	C 3-C 4	π	C 1-C 2	π^*	18.32	0.29	0.068
	N 5-C 16	π	C 1-C 2	π^*	18.90	0.40	0.080
	N 5-C 16	π	C 3-C 4	π^*	18.89	0.40	0.080
MC28	C 8-C 9	π	C 6-C 7	π^*	15.75	0.28	0.063
1.1020	C 11 - C 12	π	C 13 - C 14	π^*	16.33	0.28	0.062
	C 13 - C 14	π	C 11 - C 12	π^*	15.95	0.28	0.063
	C 17 - C 18	π	C 19	LP 1	45.95	0.14	0.091
	C 17 - C 18	π	N 5-C 16	π^*	32.60	0.23	0.089
-	C 20 - C 21	π	C 19	LP 1	44.22	0.15	0.091

$\begin{array}{c ccccccccccccccccccccccccccccccccccc$	Malays. J. Anal. Sci. Volume 29 Number 2 (2025): 1293										
$\begin{array}{c ccccccccccccccccccccccccccccccccccc$	C 20 - C 21	π	N 5-C 16	π*	31.69	0.24	0.088				
$\begin{array}{c ccccccccccccccccccccccccccccccccccc$	C 22 - C 31	π	C 19	LP 1	43.76	0.17	0.097				
$\begin{array}{c ccccccccccccccccccccccccccccccccccc$	C 22 - C 31	π	C 32 - C 33	π^*	20.10	0.27	0.069				
$\begin{array}{c ccccccccccccccccccccccccccccccccccc$	C 23 - C 24	π	C 25 - O 30	π^*	40.51	0.28	0.095				
$\begin{array}{c ccccccccccccccccccccccccccccccccccc$	C 23 - C 24	π	C 28 - N 29	π^*	33.08	0.38	0.104				
$\begin{array}{c ccccccccccccccccccccccccccccccccccc$	C 23 - C 24	π	C 32 - C 33	π^*	16.79	0.28	0.063				
$\begin{array}{c ccccccccccccccccccccccccccccccccccc$	C 32 - C 33	π	C 23 - C 24	π^*	33.33	0.31	0.091				
$\begin{array}{c ccccccccccccccccccccccccccccccccccc$	S 10	LP 2	C 6-C 7	π^*	25.12	0.26	0.073				
$\begin{array}{c ccccccccccccccccccccccccccccccccccc$	S 10	LP 2	C 8-C 9	π^*	23.17	0.26	0.071				
$\begin{array}{c ccccccccccccccccccccccccccccccccccc$	S 15	LP 2	C 11 - C 12	π^*	25.45	0.26	0.073				
$\begin{array}{c ccccccccccccccccccccccccccccccccccc$	S 15	LP 2	C 13 - C 14	π^*	22.97	0.26	0.071				
$\begin{array}{c ccccccccccccccccccccccccccccccccccc$	C 19	LP 1	C 17 - C 18	π^*	70.87	0.13	0.107				
$\begin{array}{c ccccccccccccccccccccccccccccccccccc$	C 19	LP 1	C 20 - C 21	π^*	72.72	0.13	0.107				
$\begin{array}{c ccccccccccccccccccccccccccccccccccc$	C 19	LP 1	C 22 - C 31	π^*	103.21	0.11	0.114				
$\begin{array}{c ccccccccccccccccccccccccccccccccccc$	O 26	LP 2	C 25 - O 30	π^*	50.44	0.32	0.119				
$\begin{array}{c ccccccccccccccccccccccccccccccccccc$	N 29	LP 1	C 28	RY* 1	15.65	1.10	0.118				
$\begin{array}{c ccccccccccccccccccccccccccccccccccc$	O 30	LP 1	C 25	RY* 1	14.09	1.36	0.124				
$\begin{array}{cccccccccccccccccccccccccccccccccccc$	O 30	LP 2	C 24 - C 25	σ^*	15.36	0.88	0.106				
$\begin{array}{c ccccccccccccccccccccccccccccccccccc$	O 30	LP 2	C 25 - O 26	σ^*	33.66	0.59	0.127				
$\begin{array}{cccccccccccccccccccccccccccccccccccc$	S 34	LP 2	C 22 - C 31	π^*	26.53	0.26	0.075				
$\begin{array}{cccccccccccccccccccccccccccccccccccc$	S 34	LP 2	C 32 - C 33	π*	23.33	0.26	0.070				
$\begin{array}{cccccccccccccccccccccccccccccccccccc$	N 5-C 16	π^*	C 1 - C 2	π^*	43.44	0.04	0.052				
$\begin{array}{cccccccccccccccccccccccccccccccccccc$	N 5-C 16	π^*	C 3 - C 4	π^*	44.28	0.04	0.052				
$\begin{array}{c ccccccccccccccccccccccccccccccccccc$	N 5-C 16	π^*	C 17 - C 18	π^*	136.56	0.04	0.096				
$\begin{array}{c ccccccccccccccccccccccccccccccccccc$	N 5-C 16	π^*	C 20 - C 21	π^*	147.11	0.04	0.096				
$\begin{array}{c ccccccccccccccccccccccccccccccccccc$	C 23 - C 24	π^*	C 28 - N 29	π^*	41.58	0.07	0.098				
$\begin{array}{cccccccccccccccccccccccccccccccccccc$	C 25 - O 30	π^*	C 23 - C 24	π^*	98.45	0.03	0.090				
$ \begin{array}{c ccccccccccccccccccccccccccccccccccc$	C 32 - C 33	π*	C 23 - C 24	π*	108.72	0.03	0.083				
$ \begin{array}{c ccccccccccccccccccccccccccccccccccc$	C 1-C 2	π	C 5-C 6	π^*	21.88	0.27	0.071				
$ \begin{array}{cccccccccccccccccccccccccccccccccccc$	C 3-C 4	π	C 1-C 2	π^*	22.10	0.28	0.071				
$ \begin{array}{c ccccccccccccccccccccccccccccccccccc$	C 5-C 6	π	C 1-C 2	π^*	20.02	0.28	0.067				
$ \begin{array}{c ccccccccccccccccccccccccccccccccccc$	C 5-C 6	π	C 3-C 4	π^*	21.88	0.28	0.071				
$ \begin{array}{cccccccccccccccccccccccccccccccccccc$	C 15 - C 20	π	C 16 - C 17	π^*	21.11	0.28	0.069				
$MK162 \begin{array}{cccccccccccccccccccccccccccccccccccc$	C 16 - C 17	π	C 18 - C 19	π^*	21.26	0.27	0.070				
$ \begin{array}{cccccccccccccccccccccccccccccccccccc$	C 18 - C 19	π	C 15 - C 20	π^*	21.28	0.29	0.071				
$\begin{array}{cccccccccccccccccccccccccccccccccccc$	C 18 - C 19	π	C 16 - C 17	π^*	18.48	0.29	0.065				
$C 30 - C 31 \pi C 32 - C 33 \pi^* 22.71 0.27 0.071$ $C 30 - C 31 \pi C 34 - C 39 \pi^* 22.69 0.30 0.074$	MK162 C 28 - C 29	π	C 30 - C 31	π^*	22.07	0.29	0.073				
	C 30 - C 31	π	C 32 - C 33	π^*	22.71	0.27	0.071				
$C 32 - C 33$ π $C 28 - C 29$ π^* 22.36 0.27 0.073	C 30 - C 31	π	C 34 - C 39	π^*	22.69	0.30	0.074				
	C 32 - C 33	π	C 28 - C 29	π^*	22.36	0.27	0.073				
C 34 - C 39 π C 37 - C 38 π^* 24.00 0.31 0.078	C 34 - C 39	π	C 37 - C 38	π^*	24.00	0.31	0.078				
C 35 - C 36 π C 34 - C 39 π^* 24.46 0.32 0.080	C 35 - C 36	π	C 34 - C 39	π^*	24.46	0.32	0.080				
$C 37 - C 38 \pi C 35 - C 36 \pi^* 23.73 0.31 0.078$	C 37 - C 38	π	C 35 - C 36	π^*	23.73	0.31	0.078				
C 37 - C 38 π C 42 - C 46 π* 23.58 0.31 0.076	C 37 - C 38	π	C 42 - C 46	π*	23.58	0.31	0.076				

Malays. J. Anal. Sci. Volume 29 Number 2 (2025): 1293									
	C 41 - C 43	π	C 44 - C 45	π^*	25.31	0.26	0.076		
	C 42 - C 46	π	C 44 - C 45	π*	28.00	0.26	0.078		
	C 44 - C 45	π	C 47 - C 48	π*	27.20	0.24	0.073		
	C 49 - C 50	π	C 52 - C 53	π^*	33.11	0.31	0.091		
	C 52 - C 53	π	C 54 - O 71	π*	40.53	0.27	0.095		
	C 52 - C 53	π	C 55 - N 56	π^*	32.97	0.38	0.104		
	C 60 - C 61	σ	C 69 - C 70	π*	26.75	0.18	0.066		
	C 61 - C 63	π	C 62 - C 66	π^*	54.00	0.35	0.124		
	C 62 - C 66	π	C 64 - C 65	π^*	22.34	0.34	0.080		
	C 64 - C 65	π	C 62 - C 66	π^*	20.65	0.33	0.075		
	C 69 - C 70	π	C 60 - C 61	σ^*	26.05	0.14	0.056		
	O 7	LP 2	C 5-C 6	π*	29.79	0.33	0.095		
	N 14	LP 1	C 3-C 4	π*	21.12	0.28	0.070		
	N 14	LP 1	C 28 - C 29	π*	64.93	0.29	0.126		
	O 21	LP 2	C 18 - C 19	π*	32.08	0.33	0.098		
	S 51	LP 2	C 47 - C 48	π^*	26.11	0.26	0.075		
	O 57	LP 2	C 54 - O 71	π^*	50.39	0.32	0.119		
	O 71	LP 2	C 54 - O 57	σ^*	32.92	0.59	0.126		
	C 28 - C 29	π^*	C30 - C 31	π^*	229.57	0.02	0.081		
	C 30 - C 31	π^*	C 34 - C 39	π^*	220.38	0.02	0.086		
	C 44 - C 45	π^*	C 41 - C 43	π^*	76.17	0.05	0.089		
	C 44 - C 45	π^*	C 42 - C 46	π^*	83.99	0.05	0.089		
	C 49 - C 50	π^*	C 52 - C 53	π^*	108.54	0.03	0.083		
	C 52 - C 53	π^*	C 55 - N 56	π^*	41.88	0.07	0.098		
	C 54 - O 71	π^*	C 52 - C 53	π^*	99.22	0.03	0.091		
	C 61 - C 63	π^*	C 64 - C 65	π^*	37.78	0.04	0.062		
	C 62 - C 66	π^*	C 64 - C 65	π^*	162.18	0.02	0.083		
	C 69 - C 70	π^*	C 59 - C 60	π*	84.54	0.01	0.059		
	O 57	LP 1	H 58	LP* 1	15.82	0.69	0.107		
	O 57	LP 3	H 58	LP* 1	478.36	0.64	0.495		
	O 57	LP 3	H 58	RY* 1	30.68	1.13	0.191		
	C 1 - C 6	π	C 2-C 3	π*	19.27	0.28	0.066		
	C 1-C 6	π	C 4-C 5	π*	20.91	0.28	0.069		
	C 2-C 3	π	C 1-C 6	π*	21.73	0.27	0.069		
	C 2-C 3	π	C 4-C 5	π*	20.55	0.27	0.067		
	C 4-C 5	π	C 1-C 6	π*	19.53	0.29	0.067		
M7172	C 4-C 5	π	C 2-C 3	π*	20.09	0.29	0.068		
MZ173	C 9 - C 14	π	C 10 - C 11	π* -*	18.67	0.29	0.065		
	C 9 - C 14	π	C 12 - C 13	π* -*	21.60	0.30	0.072		
	C 10 - C 11	π	C 9 - C 14	π* -*	21.63	0.28	0.070		
	C 10 - C 11	π	C 12 - C 13	π* -*	17.66	0.29	0.064		
	C 12 - C 13	π	C 9 - C 14	π* -*	19.95	0.27	0.066		
	C 12 - C 13	π	C 10 - C 11	π* I D* 1	23.03	0.27	0.071		
	C 15 - C 16	π	C 8	LP* 1	59.05	0.13	0.096		

Malays. J. Anal. Sci. Volume 29 Number 2 (2025): 1293									
C 15 - C 16	π	C 17	LP 1	40.01	0.15	0.088			
C 18 - C 19	π	C 8	LP* 1	56.61	0.13	0.096			
C 18 - C 19	π	C 17	LP 1	38.52	0.15	0.088			
C 21 - C 22	π	C 17	LP 1	43.26	0.17	0.096			
C 21 - C 22	π	C 23 - C 24	π^*	20.30	0.27	0.069			
C 23 - C 24	π	C 21 - C 22	π^*	13.37	0.29	0.057			
C 23 - C 24	π	C 26 - C 27	π^*	33.42	0.31	0.091			
C 26 - C 27	π	C 23 - C 24	π^*	16.70	0.28	0.063			
C 26 - C 27	π	C 28 - O 33	π^*	40.91	0.27	0.096			
C 26 - C 27	π	C 31 - N 32	π^*	33.39	0.37	0.104			
N 7	LP 1	C 8	LP* 1	145.46	0.15	0.159			
N 7	LP 1	C 4-C 5	π^*	21.65	0.29	0.071			
N 7	LP 1	C 9 - C 14	π^*	21.68	0.29	0.071			
C 8	LP*1	C 15 - C 16	π^*	55.36	0.15	0.102			
C 8	LP*1	C 18 - C 19	π^*	56.79	0.15	0.102			
C 17	LP 1	C 15 - C 16	π^*	77.79	0.13	0.109			
C 17	LP 1	C 18 - C 19	π^*	79.99	0.13	0.109			
C 17	LP 1	C 21 - C 22	π^*	105.05	0.12	0.115			
S 25	LP 2	C 21 - C 22	π^*	26.39	0.26	0.075			
S 25	LP 2	C 23 - C 24	π^*	22.95	0.26	0.070			
O 29	LP 2	C 28 - O 33	π^*	50.22	0.32	0.119			
O 33	LP 2	C 8 - O 29	σ^*	33.69	0.59	0.127			
C 9-C 14	π^*	C 12 - C 13	π^*	231.44	0.01	0.084			
C 23 - C 24	π^*	C 26 - C 27	π^*	109.39	0.03	0.083			
C 26 - C 27	π^*	C 31 - N 32	π^*	42.99	0.07	0.098			
C 28 - O 33	π*	C 26 - C 27	π*	99.46	0.03	0.090			
C 1-C 2	π	C 3-C 4	π^*	24.03	0.30	0.076			
C 1-C 2	π	C 5-C 6	π^*	23.50	0.29	0.075			
C 3-C 4	π	C 1-C 2	π^*	20.37	0.31	0.072			
C 3-C 4	π	C 5-C 6	π^*	20.52	0.29	0.071			
C 5-C 6	π	C 1-C 2	π^*	22.11	0.32	0.075			
C 5-C 6	π	C 3-C 4	π^*	21.62	0.32	0.074			
C 8-C 19		C 15 - C 16	π^*	20.45	0.31	0.073			
C 8-C 19		C 17 - C 18	π*	23.97	0.32	0.079			
MZ175 C 9-C 14		C 10 - C 11	π^*	21.29	0.32	0.073			
C 9-C 14		C 12 - C 13	π^*	23.10	0.32	0.077			
C 12 - C 13		C 9 - C 14	π*	23.22	0.29	0.074			
C 12 - C 13		C 10 - C 11	π^*	25.31	0.30	0.078			
C 17 - C 18		C 20	LP* 1	57.18	0.15	0.099			
C 17 - C 18		C 8 - C 19	π^*	22.77	0.29	0.073			
C 17 - C 18		C 15 - C 16	π^*	24.29	0.30	0.078			
C 21 - C 22		C 20	LP* 1		0.16	0.102			
C 21 - C 22		C 23	LP 1	49.73	0.15	0.098			
C 24 - C 25	π	C 20	LP* 1	52.70	0.17	0.102			

Malays	Malays. J. Anal. Sci. Volume 29 Number 2 (2025): 1293								
C 24 - C 25	π	C 23	LP 1	46.53	0.16	0.096			
C 26 - C 27	π	C 23	LP 1	31.48	0.17	0.084			
C 26 - C 27	π	C 28 - O 31	π^*	37.75	0.27	0.092			
C 26 - C 27	π	C 32 - N 33	π^*	29.93	0.38	0.099			
N 7	LP 1	C 5-C 6	π^*	42.93	0.31	0.103			
N 7	LP 1	C 8-C 19	π^*	45.79	0.31	0.107			
N 7	LP 1	C 9-C 14	π^*	42.89	0.31	0.104			
C 20	LP*1	C 17 - C 18	π^*	70.33	0.15	0.112			
C 20	LP*1	C 21 - C 22	π^*	67.51	0.15	0.114			
C 20	LP*1	C 24 - C 25	π^*	71.03	0.14	0.114			
C 23	LP 1	C 21 - C 22	π^*	74.38	0.16	0.119			
C 23	LP 1	C 24 - C 25	π^*	75.47	0.15	0.117			
C 23	LP 1	C 26 - C 27	π^*	91.50	0.14	0.125			
O 29	LP 2	C 28 - O 31	π^*	47.36	0.31	0.112			
O 31	LP 2	C 28 - O 29	σ^*	32.88	0.57	0.124			
C 5-C 6	π^*	C 1-C 2	π^*	230.24	0.02	0.092			
C 5-C 6	π^*	C 3-C 4	π^*	268.08	0.01	0.088			
C 8-C 19	π^*	C 15 - C 16	π^*	327.97	0.01	0.089			
C 8-C 19	π^*	C 17 - C 18	π^*	268.94	0.02	0.093			
C 9-C 14	π^*	C 10 - C 11	π^*	289.42	0.01	0.088			
C 9-C 14	π^*	C 12 - C 13	π^*	191.30	0.02	0.094			
C 26 - C 27	π^*	C 32 - N 33	π^*	29.53	0.07	0.096			
C 28 - O 31	π*	C 26 - C 27	π*	74.80	0.04	0.088			

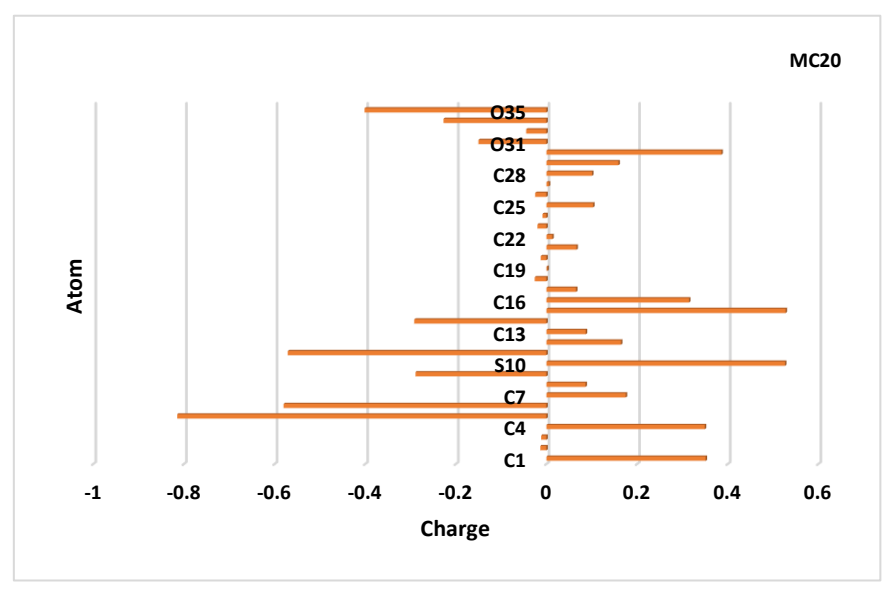
 $\textbf{Table 3.} \ Dipole \ moment \ parameters \ and \ polarizability \ optimized \ with \ DFT \ B3LYP/6-31G$

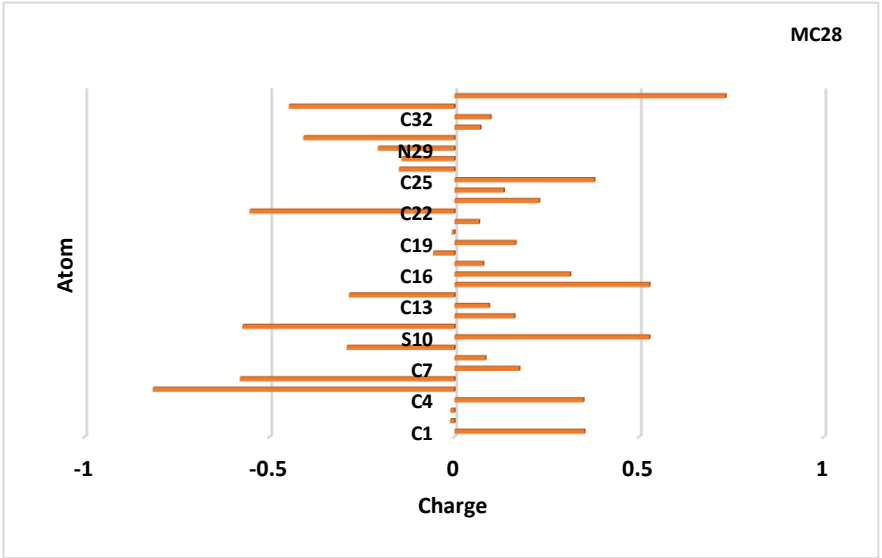
	MC20		MC28		MK	MK162		MZ173		175
	a.u	esu (10 ⁻²⁴)	a.u	esu (10 ⁻²⁴)	a.u	esu (10 ⁻²⁴)	a.u	esu (10 ⁻²⁴)	a.u	esu (10 ⁻²⁴)
α_{xx}	541,389	80,233	414,011	61,356	1669,501	247,420	407,760	60,430	362,749	53,759
α_{xy}	148,679	22,034	67,797	10,047	-302,374	-44,811	130,066	19,275	-154,011	-22,824
α_{yy}	505,903	74,974	611,652	90,646	815,921	120,919	657,517	97,444	673,794	99,856
α_{xz}	-0,101	-0,014	-8,782	-1,301	-19,733	-2,924	-41,622	-6,168	9,368	1,388
α_{yz}	-78,466	-11,628	-105,360	-15,614	-55,475	-8,221	-117,265	-17,378	-236,008	-34,976
αzz	202,073	29,947	201,279	29,829	646,884	95,868	189,320	28,057	258,559	38,318
<a>>	416,455	61,718	408,981	60,611	1044,102	154,735	418,199	61,977	431,701	63,978
μx	1,908	****	-0,437	****	-3,519	****	0,280	****	0,193	****
μу	0,709	****	1,985	****	2,922	****	3,211	****	-2,711	****
μ_z	-0,369	****	-1,073	****	-0,894	****	-0,753	****	1,768	****
μtot	2,069	****	2,299	****	4,661	****	3,311	****	3,242	****

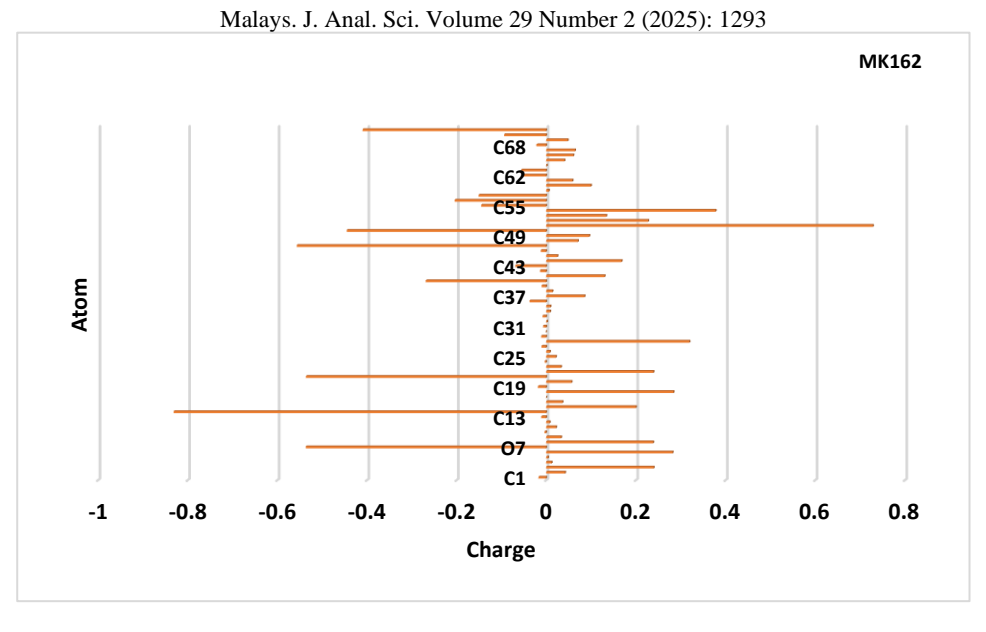
Mulliken atomic charges

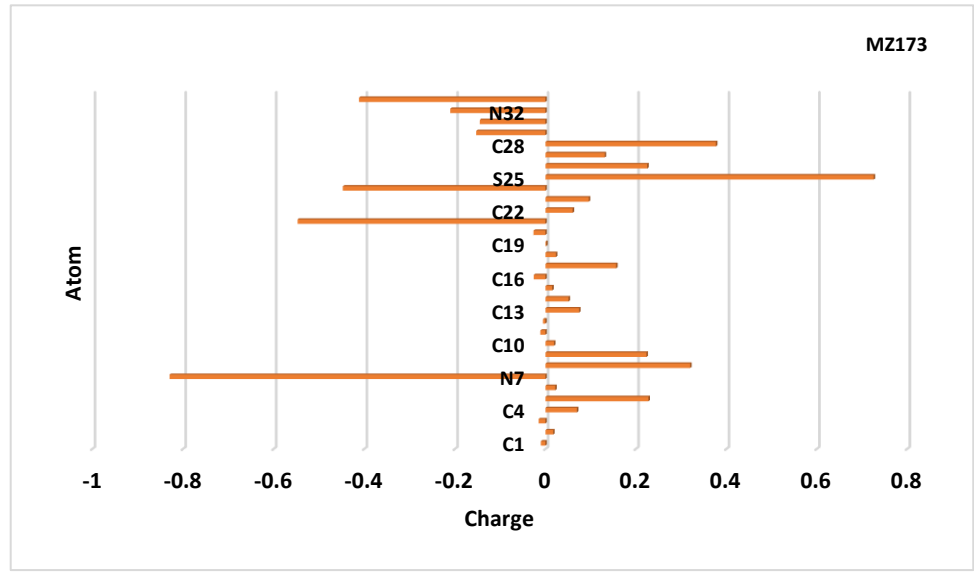
The calculation of mulliken atomic charges has an appreciable utility in the application of quantum mechanical calculations to molecular systems, in fact atomic charges have an influence on the dipole moment, molecular polarization, electronic structure and other properties of molecular systems, in addition the distribution of charges on atoms suggests the formation of pairs of donors and acceptors involving the transfer of charge in the molecule [38]. The mulliken atomic charges of the molecules MC20, MC28, MK162, MZ173 and MZ175 are optimized by the B3LYP method using

the 6-31G base set. The distribution of the charges on the examined molecules are drawn in the figure 3, the sulfur atoms indicate the greatest value of the positive charge (S10, S15, S34, S51 and S25), while the carbon atoms (C6, C9, C11, C14, C22, C33, C47 and C50) linked directly to sulfur carry the most negative charges, the nitrogen and oxygen atoms carry negative charges, it is found that the carbon atoms closest to sulfur are the most electronegative this may be due to the delocalization of electronic pairs and sulfur.









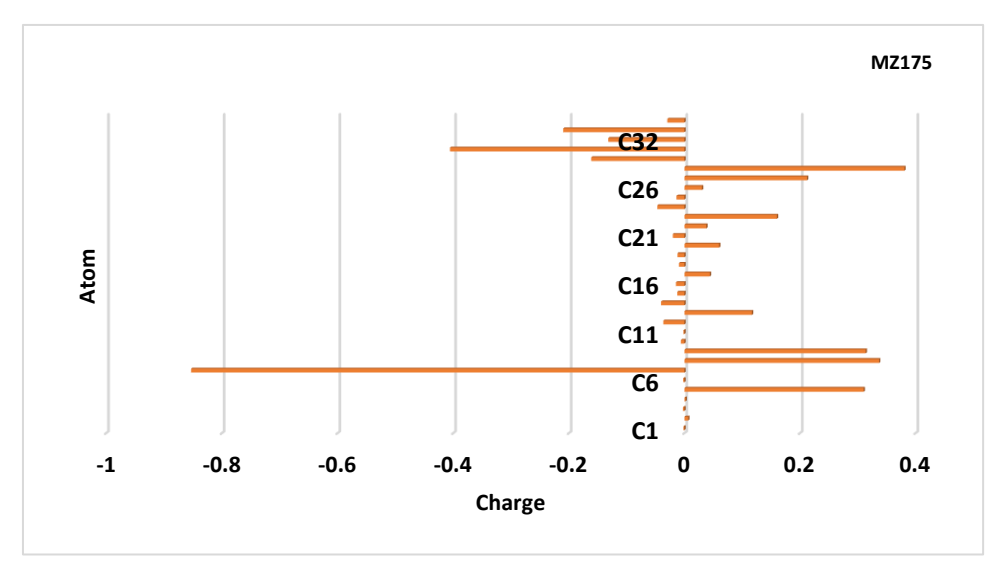


Figure 3. The mulliken charge analysis of the molecules MC20, MC28, MK162, MZ173 and MZ175

 Table 4. First-order hyperpolarizability optimized with DFT B3LYP/6-31G

	MC20		MC28		MK	MK162		MZ173		MZ175	
	a.u	esu (10 ⁻²⁴)	a.u	esu (10 ⁻²⁴)	a.u	esu (10 ⁻²⁴)	a.u	esu (10 ⁻²⁴)	a.u	esu (10 ⁻²⁴)	
βxxx	-5379,579	-46475,801	-873,500	-7546,435	177288,350	1531647,25	-1340,047	-11577,069	-1329,675	-11487,468	
βхху	-6442,154	-55655,702	-1797,685	-15530,745	-48823,206	-421798,323	-4387,769	-37907,254	5214,346	45048,307	
βyyz	-7017,469	-60626,024	-4588,306	-39639,757	13419,711	115936,914	-9629,544	-83192,522	-15225,361	-131536,463	
βxyz	-7258,191	-62705,691	-9299,519	-80341,341	-3786,819	-32715,466	-16137,692	-139418,36	37510,051	324060,586	
βxxz	1596,100	13789,192	536,473	4634,759	5458,203	47155,054	1171,499	10120,935	-2240,354	-19355,094	
βууу	1562,703	13500,663	1194,528	10319,891	-1575,919	-13614,842	2504,573	21637,761	6195,654	53526,115	
βzzz	1635,834	14132,461	2510,525	21689,186	344,789	2978,739	4127,649	35660,003	-14655,613	-126614,24	
βxzz	-304,865	-2633,825	-302,892	-2616,778	150,730	1302,206	-630,504	-5447,115	-2449,276	-21160,035	
βyzz	-343,118	-2964,307	-657,990	-5684,577	-274,795	-2374,036	-1004,531	-8678,450	5584,475	48245,962	
βхуу	57,360	495,551	151,411	1308,085	-1470,906	-12707,601	234,317	2024,342	-2021,341	-17462,975	
β_{tot}	8559,766	73950,387	2239,800	19350,312	184125,384	1590714,43	5486,875	47402,761	36799,938	317925,705	

Non-linear optical properties

The calculations of the dipole moment, the polarizability and the first-order hyperpolarizability are taught on the non-linear optical properties of the molecule [39]. The values calculated after transformation into electrostatic units (esu) for the molecules MC20, MC28, MK162, MZ173 and MZ175 are illustrated in the Tables 2 and 3. The high values of the dipole moment, the polarizability and the first-order hyperpolarizability show that the NLO properties are very active (Table 4). However, the higher total value of μ is obtained for the MK162 molecule. Consequently, the μ_{tot} values of the studied molecules are classified in the following descending order: $\mu_{tot}(MK162) > \mu_{tot}(MZ173) >$ $\mu_{tot}(MZ175) > \mu_{tot}(MC28) > \mu_{tot}(MC20)$. The maximum value of the polarizability is obtained for the molecule MK162, consequently the values of $<\alpha>$ are classified in the following descending $<\alpha>(MK162)>$ $<\alpha>(MZ175)>$ order: $\langle \alpha \rangle (MZ173) \rangle \langle \alpha \rangle (MC20) \rangle \langle \alpha \rangle (MC28)$. The of the first-order maximum value hyperpolarizability is obtained for the MK162 molecule, therefore the β_{tot} values have been classified in the following decreasing order: $\beta_{tot}(MK162) > \beta_{tot}(MZ175) > \beta_{tot}(MC20) >$ $\beta_{tot}(MZ173) > \beta_{tot}(MC28)$. All the values of the optimized parameters are larger than that of the urea molecule which is one of the molecular systems most used to compare the NLO properties of organic compounds as a threshold value (urea: μ =1.3732 Debaye, α =3.8312×× A^{o3} and β $=3.7289 \times 10^{-31} \text{cm}^{5}/\text{esu}$) obtained by B3LYP/6-31G(d) [40]. The high values of the optimized parameters affirm that the molecules studied are candidate molecules to be NLO materials.

Conclusion

This investigation reveals remarkable nonlinear optical activity in MC20, MC28, MK162, MZ173, and MZ175. Through meticulous calculations, we have observed elevated dipole moments, polarizability, and first-order hyperpolarizability values for these molecules, positioning them as promising candidates for applications in nonlinear optics materials. Significantly, the optimized parameters for these molecules outperform those of the reference urea molecule, underscoring their substantial potential for practical use in advanced nonlinear optics applications.

The detailed exploration of structural geometries, Natural Bond Orbital (NBO) analyses, and NLO characteristics has provided valuable insights into the electron density dispersion across these molecules. The minor energy distinctions between the computed Highest Occupied Molecular Orbital (HOMO) and Lowest Unoccupied Molecular Orbital (LUMO) levels facilitate efficient

intramolecular charge transfer, indicating the ease and speed with which this process occurs. The NBO analysis further confirms the good electron density delocalization in all four studied compounds, leading to intense and successful intramolecular charge transfer. Notably, our findings position these molecules as superior to urea in terms of optimized NLO properties.

This study raises intriguing questions for future exploration. The investigation into the thermo-electric properties of the studied thiophene-based materials and their stability in solar cell systems presents avenues for further research. Addressing these questions in subsequent works holds the potential to enhance our understanding and utilization of these molecules in diverse applications, extending beyond their roles as excellent candidates for NLO materials to promising materials for organic photovoltaic systems [1].

References

- 1. Kang, D., Li, R., Cao, S., and Sun, M. (2021). Nonlinear optical microscopies: Physical principle and applications. *Applied Spectroscopy Reviews*, 56(1):52-66.
- 2. Tian, T., Wang, Y., Zhang, W., Wang, B., and Fan, C. (2020). DAST optical damage tolerance enhancement and robust lasing via supramolecular strategy. *ACS Photonics*. 7(8): 2132-2138.
- Mohan, M.K., Ponnusamy, S., and Muthamizhchelvan, C. (2018);. Spectral, optical, etching, second harmonic generation (SHG) and laser damage threshold studies of nonlinear optical crystals of L-Histidine bromide. *Applied Surface Sciences*, 449: 92-95
- 4. Zhang, B., Shi, G., Yang, Z., Zhang, F., Pan, S. (2017), Fluorooxoborates: Beryllium-free deep-ultraviolet nonlinear optical materials without layered growth. *Angewandte Chemie International Edition*, 56: 3916–3919
- Pourebrahimi, S., Pirooz, M., Visscher, A. (2024). DFT-assisted design of curcumin-based donor-π-bridge-acceptor molecular structures: advancing non-linear optical materials and sustainable organic solar cells. *Journal of Molecular Structure*, 1316.
- 5. Janjua, M. R. S. A., Liu, C.G., Guan, W., Zhuang, J., Muhammad, S., Yan, L.K., and Su, Z.M. (2009) Prediction of remarkably large second-order nonlinear optical properties of organoimidosubstituted hexamolybdates. *Journal Materials Chemistry A*, 113: 3576-3587.
- 7. Muhammad, S., Xu, H., Liao, Y., Kan, Y., and Su, Z. (2009). Quantum mechanical design and structure of the Li@B10H14

- basket with a remarkably enhanced electrooptical response. *Journal American Chemical Society*, 131: 11833-11840.
- 8. Bullo, S., Jawaria, R., Faiz, I., Shafiq, I., Khalid, M., Asghar, M. A., and Perveen, S. (2023). Efficient synthesis, spectroscopic characterization, and nonlinear optical properties of novel salicylaldehyde-based thiosemicarbazones: experimental and theoretical studies. *ACS Omega*, 8(15): 13982-13992.
- Srinivas, K., Kumar, C. R., Reddy, M. A., Bhanuprakash, K., Rao, V. J., and Giribabu, L. (2011). D-π-A organic dyes with carbazole as donor for dye-sensitized solar cells. Synthetic Metals, 161(1-2): 96-105.
- Azaid, A., Alaqarbeh, M., Abram, T., Raftani, M., Kacimi, R., Khaddam, Y., and Bouachrine, M. (2024). D-π-A push-pull chromophores based on N, N-Diethylaniline as a donor for NLO applications: effects of structural modification of π-linkers. *Journal* of Molecular Structure, 1295:136602.
- 11. Zhao, Y., and Truhlar, D. G. (2008). The M06 suite of density functionals for main group thermochemistry, thermochemical kinetics, noncovalent interactions, excited states, and transition elements: two new functionals and systematic testing of four M06-class functionals and 12 other functionals. *Theoretical Chemistry Account*, 120: 215-241.
- Khan, M. U., Fatima, A., Nadeem, S., Abbas, F., and Ahamad, T. (2023). Impact of π-linkers modifications on tuning nonlinear optical amplitudes of pyridoquinazolinone-based aromatic dyes: A rational entry to novel D-π-A NLO materials. *Polycyclic Aromatic Compounds*, 2023: 1-31.
- Khalid, M., Khan, M. U., Shafiq, I., Hussain, R., Ali, A., Imran, M., and Akram, M. S. (2021). Structural modulation of π-conjugated linkers in D-π-A dyes based on triphenylamine dicyanovinylene framework to explore the NLO properties. *Royal Society Open Science*. 8(8): 210570..
- 14. Khan, M. U., Ibrahim, M., Khalid, M., Braga, A. A. C., Ahmed, S., and Sultan, A. (2019). Prediction of second-order nonlinear optical properties of D–π–A compounds containing novel fluorene derivatives: A promising route to giant hyperpolarizabilities. *Journal of Cluster Science*, 30: 415-430.
- Etabti, H., Fitri, A., Benjelloun, A. T., Benzakour, M., and Mcharfi, M. (2023).
 Designing and theoretical study of benzocarbazole-based D-π-D type small molecules donor for organic solar

- cells. Journal of Molecular Graphics and Modelling, 121: 108455.
- Khalid, M., Ali, A., Jawaria, R., Asghar, M. A., Asim, S., Khan, M. U., and Akram, M. S. (2020). First principles study of electronic and nonlinear optical properties of A–D–π–A and D–A–D–π–A configured compounds containing novel quinoline–carbazole derivatives. *RSC Advances*, 10(37): 22273-22283.
- 17. Zouitina, S., El Azze, S., Bensemlali, M., Faqir, M., and Tounsi, A. (2022). First-principles study of nonlinear optical and electronic properties of A-π-D-π-A configured compounds with novel oligothiophenes. *Materials Science for Energy Technologies*. 5: 473-480.
- 18. Shen, D., Chen, W. C., Lo, M. F., and Lee, C. S. (2021). Charge-transfer complexes and their applications in optoelectronic devices. *Materials Today Energy*, 20: 100644.
- Lee, M. W., Kim, J. Y., Lee, H. G., Cha, H. G., Lee, D. H., and Ko, M. J. (2021). Effects of structure and electronic properties of D-π-A organic dyes on photovoltaic performance of dye-sensitized solar cells. *Journal of Energy Chemistry*, 54: 208-216.
- 20. Qu, W., Gao, Z., Fan, X., Tian, X., Wang, H., and Wei, B. (2022). Organic fluorescent compounds with twisted D-π-A molecular structure and acidochromic properties. *Journal of Molecular Structure*, 1260: 132831.
- Ramalingam, A., Sambandam, S., Medimagh, M., Al-Dossary, O., Issaoui, N., and Wojcik, M. J. (2021). Study of a new piperidone as an anti-Alzheimer agent: Molecular docking, electronic and intermolecular interaction investigations by DFT method. *Journal of King Saud University-Science*, 33(8): 101632.
- 22. Frisch, M. J., Trucks, G. W., Schlegel, H. B., Scuseria, G. E., Robb, M., Cheeseman, J. R., ... and Fox, A. D. (2009). Gaussian Inc. *Wallingford Ct*, 2009.
- 23. Yanai, T., Tew, D. P., and Handy, N. C. (2004). A new hybrid exchange–correlation functional using the Coulomb-attenuating method (CAM-B3LYP). *Chemical Physics Letters*, 393(1-3): 51-57.
- 24. Dennington, R. D. I. I., Keith, T. A., and Millam, J. M. (2016). Gauss View, version 6.0. 16. Semichem Inc Shawnee Mission KS.
- Avcı, D. (2011). Second and third-order nonlinear optical properties and molecular parameters of azo chromophores: Semiempirical analysis. Spectrochimica Acta Part A: Molecular and Biomolecular Spectroscopy, 82(1): 37-43.

- Azaid, A., Raftani, M., Alaqarbeh, M., Kacimi, R., Abram, T., Khaddam, Y., and Bouachrine, M. (2022). New organic dyesensitized solar cells based on the D–A–π–A structure for efficient DSSCs: DFT/TD-DFT investigations. *RSC Advances*, 12(47): 30626-30638.
- Kadam, M. M., Patil, D., and Sekar, N. (2018). 4-(Diethylamino) salicylaldehyde based fluorescent Salen ligand with redshifted emission—A facile synthesis and DFT investigation. *Journal of Luminescence*, 204: 354-367.
- 28. Arulaabaranam, K., Muthu, S., Mani, G., and Geoffrey, A. B. (2021). Speculative assessment, molecular composition, PDOS, topology exploration (ELF, LOL, RDG), ligand-protein interactions, on 5-bromo-3-nitropyridine-2-carbonitrile. *Heliyon*, 7(5): e07061.
- Kores, J. J., Danish, I. A., Sasitha, T., Stuart, J. G., Pushpam, E. J., and Jebaraj, J. W. (2021). Spectral, NBO, NLO, NCI, aromaticity and charge transfer analyses of anthracene-9, 10-dicarboxaldehyde by DFT. *Heliyon*, 7(11): e08377.
- Sharma, K., Melavanki, R., Patil, S. S., Kusanur, R., Patil, N. R., and Shelar, V. M. (2019). Spectroscopic behavior, FMO, NLO and NBO analysis of two novel aryl boronic acid derivatives: Experimental and theoretical insights. *Journal of Molecular Structure*, 1181: 474-487.
- 31. Khan, B., Khalid, M., Shah, M. R., Tahir, M. N., Asif, H. M., Aliabad, H. A. R., and Hussain, A. (2020). Synthetic, spectroscopic, SC-XRD and nonlinear optical analysis of potent hydrazide derivatives: a comparative experimental and DFT/TD-DFT exploration. *Journal of Molecular Structure*, 1200: 127140.
- 32. Meenatchi, V., Cheng, L., Han, S. S. (2023). Twisted intramolecular charge transfer, nonlinear optical, antibacterial activity, and DFT analysis of ultrasound processed (E)-N'-(4-isopropylbenzylidene) nicotinohydrazide. *Journal of Molecular Liquids*, 376: 121489.
- 33. Ahmed, Z. K., Ermiş, T., and Ermiş, E. (2024). Theoretical and experimental study on (E)-N'-(2-hydroxy-5-(thiophen-3-yl) benzylidene) benzohydrazide compound: Its optimization with DFT and Fuzzy logic approach (FLA), structural and spectroscopic investigation, HOMO-LUMO,

- MEP, atomic charge, and NBO analysis. *Journal of Molecular Structure*, 1315: 138829.
- 34. Ali, B., Khalid, M., Asim, S., Usman Khan, M., Iqbal, Z., Hussain, A., Hussain, R., Ahmed, S., Ali, A., Hussain, A., Imran, M., Assiri, M. A., Fayyaz ur Rehman, M., Wang, C., and Lu, C. (2021). Key electronic, linear and nonlinear optical properties of designed disubstituted quinoline with carbazole compounds. *Molecules*, 26(9): 2760.
- Saral, A., Manikandan, A., Javed, S., and Muthu, S. (2024). Vibrational spectra, molecular level solvent interaction, stabilization, donor-acceptor energies, thermodynamic, non-covalent interaction electronic behaviors of Methoxyisoquinoline-anti tubercular agent. Chemical Physics Impact, 8: 100392.
- Ojha, J. K., Ramesh, G., and Reddy, B. V. (2023). Structure, chemical reactivity, NBO, MEP analysis and thermodynamic parameters of pentamethyl benzene using DFT study. *Chemical Physics Impact*, 7: 100280.
- 37. Sagir, M., Mushtaq, K., Khalid, M., Khan, M., Tahir, M. B., and Braga, A. A. (2023). Exploration of linear and third-order nonlinear optical properties for donor–π-linker–acceptor chromophores derived from ATT-2 based non-fullerene molecule. *RSC Advances*, 13(45): 31855-31872.
- Shivaleela, B., Shivraj, G. G., and Hanagodimath, S. M. (2023). Estimation of dipole moments by Solvatochromic shift method, spectroscopic analysis of UV– Visible, HOMO-LUMO, ESP map, Mulliken atomic charges, NBO and NLO properties of benzofuran derivative. *Results in Chemistry*, 6:101046.
- 39. Olea-Amezcua, M. A., Castellanos-Águila, J. E., and Trejo-Durán, M. (2022). Theoretical study of the non-linear optical properties of colloids formed by different Au and Ag nanocluster morphologies and molecular organic solvents. *Journal of Molecular Liquids*, 359: 119307.
- Singh, P., Kumar, A., Gupta, A., and Patil, P. S. (2022). Spectroscopic investigation and density functional theory prediction of first and second order hyperpolarizabilities of 1-(4-bromophenyl)-3-(2, 4-dichlorophenyl)-prop-2-en-1-one. *Journal of Molecular Structure*, 1269: 133807.